

Investigating the large-scale environment of wide-angle tailed radio galaxies in the local Universe

V. Missaglia^{1,2,3,4}, A. Paggi^{1,3,4,5}, F. Massaro^{1,3,4,5}, A. Capetti³, R. D. Baldi⁶, R. P. Kraft⁷, M. Paolillo⁸, A. Tramacere⁹, R. Campana¹⁰, and I. Pillitteri¹¹

¹ Dipartimento di Fisica, Università degli Studi di Torino, via Pietro Giuria 1, 10125, Torino, Italy

² Institute of Astrophysics, Foundation for Research and Technology - Hellas, Voutes, 7110 Heraklion, Greece

³ INAF - Osservatorio Astrofisico di Torino, via Osservatorio 20, 10025, Pino Torinese, Italy

⁴ Istituto Nazionale di Fisica Nucleare, Sezione di Torino, 10125, Torino, Italy

⁵ Consorzio Interuniversitario per la Fisica Spaziale, via Pietro Giuria 1, 10125, Torino, Italy

⁶ INAF - Istituto di Radioastronomia, via Piero Gobetti 101, 40129, Bologna, Italy

⁷ Center for Astrophysics | Harvard & Smithsonian, 60 Garden Street, 02138, Cambridge (MA), USA

⁸ Dipartimento di Fisica "Ettore Pancini", Università di Napoli Federico II, via Cintia, 80126, Napoli, Italy

⁹ University of Geneva, Chemin d'Ecogia 16, Versoix, CH-1290, Switzerland

¹⁰ INAF/OAS, via Piero Gobetti 101, 40129, Bologna, Italy

¹¹ INAF - Osservatorio Astronomico di Palermo "G. S. Vaiana", Piazza del Parlamento 1, 90134, Palermo, Italy

April 20, 2023

ABSTRACT

We present a statistical analysis of the large-scale (up to 2 Mpc) environment of an homogeneous and complete sample, both in radio and optical selection, of wide-angle tailed radio galaxies (WATs) in the local Universe (i.e., with redshifts $z \lesssim 0.15$). The analysis is carried out using the parameters obtained from cosmological neighbors within 2 Mpc of the target source. Results on WATs large-scale environments are then compared with that of Fanaroff-Riley type I (FR Is) and type II (FR IIs) radio galaxies, listed in two others homogeneous and complete catalogs, and selected with the same criterion adopted for the WATs catalog. We obtain indication that at low redshift WATs inhabit environments with a larger number of galaxies than that of FR Is and FR IIs. In the explored redshift range, the physical size of the galaxy group/cluster in which WATs reside appears to be almost constant with respect to FR Is and FR IIs, being around 1 Mpc. From the distribution of the concentration parameter, defined as the ratio between the number of cosmological neighbors lying within 500 kpc and within 1 Mpc, we conclude that WATs tend to inhabit the central region of the group/cluster in which they reside, in agreement with the general paradigm that WATs are the cluster BCG.

Key words. surveys – methods: statistical – galaxies: active galaxies: clusters: general – galaxies: jets – radio continuum: galaxies.

1. Introduction

Extragalactic extended radio sources have been classified taking into account the relative positions of their high and low brightness regions, that are found to be correlated with the luminosity of these sources (Fanaroff & Riley 1974): edge-darkened radio sources were classified as Fanaroff-Riley type I (FR Is), while edge-brightened as type II (FR IIs). A summary of the structural properties of extended extragalactic radio sources is reported by Miley (1980). The FR I/FR II dichotomy reflects the different cosmological evolution of these two classes (Longair 1971), and it is debated if there is a link between accretion modes and radio morphology (Best & Heckman 2012). This sources appear also to be related with the large-scale environment where they reside (see e.g. Worrall & Birkinshaw 2000). Many different methods have been already used to investigate the large-scale environment of radio sources. Thanks to multifrequency observations and redshift estimates, it has been possible to remove unrelated galaxies and so improving the reliability of the analysis (Best 2004). In the optical range, the Sloan Digital Sky Survey (SDSS, York et al. 2000) has expanded our knowledge of galaxy properties, such as luminosities, morphologies, star-formation rates and nuclear activity, and how this properties depend upon the en-

vironment that a galaxy inhabits. This can place important constraints on models of galaxy formation and evolution, and allows the intrinsic properties of the galaxies to be separated from those that have been externally induced.

Studying the environment of FR Is and FR IIs on the megaparsec scale, it was found that FR Is generally inhabit galaxy-rich environments, being members of groups or galaxy clusters, while FR IIs tend to be more isolated as shown, for example, in Zirbel (1997). There are however some well known exceptions, such as Cygnus A (Carilli & Barthel 1996).

The environments of powerful radio sources have been widely studied (see e.g., Prestage & Peacock 1988; Hill & Lilly 1991) up to a $z \sim 0.5$. From the estimate of the galaxy density around these sources, it has been concluded that there is no strong statistical evidence for a difference in the environments hosting FR Is and FR IIs, but at low-redshift ($z < 0.5$) the environments appear less galaxy-rich than that of the counterparts of same radio power at high-redshift.

Another class of radio galaxies are the wide-angle tailed radio galaxies (WATs) that show the so-called “jet-hotspot-lobe transition”: there are bright hotspots (called “warmspots”) closer to their radio core with respect to FR IIs and with extended radio plumes beyond them (O’Donoghue et al. 1990). The gen-

eral morphology of WATs (firstly classified by [Owen & Rudnick 1976](#)) suggests that these sources interact significantly with the surrounding medium: these sources show bent tails as the result of the ram pressure due to the relative motion between the radio source and intracluster medium (ICM; see e.g. simulations in [Massaglia et al. 2019](#)). WATs are normally found in galaxy cluster and are in general associated with the brightest cluster galaxy (BCG; see e.g. [Burns 1981](#)). This implies that WATs can be found in merging systems, as shown in [Gómez et al. \(1997\)](#) via *ROSAT* X-ray data, or relaxed systems showing “sloshing” of the central ICM due to cluster minor mergers ([Ascasibar & Markevitch 2006](#)). WATs have proven to be reliable tracers of high-density environments up to high redshifts (see e.g. [Giacintucci & Venturi \(2009\)](#)) and may be therefore used as probes of the presence of the ICM. In the already cited work by [Burns \(1981\)](#), VLA 20-cm observations of the WAT 1919+479 (4C 47.51) are presented. The author discuss the morphology, polarization, environment and nature of the galaxy cluster hosting the radio source. The author also highlight that with X-ray observations it is possible to support the contention that the cluster around the WAT is gas rich.

As shown by [Wing & Blanton \(2011\)](#) through SDSS and Faint Images of the Radio Sky at Twenty Centimeters (FIRST, [Becker et al. 1995](#)) data, bent radio sources are more often found in galaxy clusters than non-bent radio sources, and therefore the authors point out that a radio-selected galaxy cluster sample can be obtained classifying bent radio sources from their radio morphology and then looking for their optical counterpart. In [Garon et al. \(2019\)](#), the authors investigate the effect of the cluster environment on the morphology of the sources, presenting bent sources properties (e.g spatial distribution of radio galaxies around clusters and bending angle as a function of cluster mass or pressure) selected from the Radio Galaxy Zoo project catalog ([Banfield et al. 2015](#)). The results show that the bending is higher in sources near the center of the cluster, but the authors cannot draw firm conclusions on the radio morphology of BCGs hosted in disturbed clusters.

In the literature, WATs and bent double radio sources environments have been studied both at low ($z \sim 0.2$) and mid-redshift ($z > 0.2$). [Blanton et al. \(2001\)](#) presented observations of a complete, magnitude-limited sample of 40 radio galaxies from the VLA FIRST survey, part of a larger sample of bent-double radio sources at moderate redshift. The most interesting result is that $\sim 46\%$ of the sources in the sample are associated with groups, some of them being poor groups. The high-redshift Clusters Occupied by Bent Radio AGN (COBRA) Survey ([Blanton et al. 2015](#)) uses bent radio sources as tracers of distant galaxy clusters, on the assumption that, as shown at low-redshift, these sources are good tracers of high-density environments.

[Smolčić et al. \(2007\)](#), having identified a complex galaxy cluster system in the COSMOS field via a WAT, used optical and X-ray data to investigate its host environment. The cluster shows evidence for subclustering, both in diffuse X-ray emission and in the spatial distribution of galaxies found from the optical analysis applying the Voronoi tessellation-based approach.

In this paper, extending the analysis of the large-scale environment to a complete and homogeneous (both in luminosity and redshift) sample of WATs restricted to the local Universe (i.e., source redshifts $z_{src} \leq 0.15$) we can prove if WATs environment differs from that of FR Is and FR IIs from the catalogs FRICAT and FRIICAT. WATs used in this work are listed in the WATCAT ([Missaglia et al. 2019](#), details of the catalogs are described in Section 2). A similar analysis is reported in [Massaro et al. \(2019\)](#) in which the authors presented the results of the analysis of the

large-scale environment of FR I and FR II radio galaxies from the same catalogs we use here. [Massaro et al. \(2019\)](#) concluded that radio galaxies, independently of their radio (FR I vs. FR II) classification, tend to inhabit galaxy-rich large-scale environments with similar richness.

Results from previous cited works, even if for samples at higher z with respect to that of the WATCAT, show that bent radio morphology is used to identify and characterize the environment in which the bent sources are hosted. For this reason, in this work we have defined parameters that will be used to characterize the environment in which WATCAT sources lies.

The paper is organized as follows. In § 2 we briefly describe the samples used to carry out our analysis, while in § 3 we provide a brief description of the cosmological neighbors and several ambient parameters obtainable from their distribution. Then § 5 is devoted to the results of the statistical analysis of the environment of WATs. Finally, summary and conclusions are given in § 6. In Appendix A we report values of the parameters obtained from the cosmological neighbors of WATs.

Hereinafter, we adopt cgs units for numerical results and we assume a flat cosmology with $H_0=69.6 \text{ km s}^{-1} \text{ Mpc}^{-1}$, $\Omega_M=0.286$ and $\Omega_\Lambda=0.714$ ([Bennett et al. 2014](#)), unless otherwise stated. Thus, according to these cosmological parameters, in the z range of the WATCAT, $1''$ corresponds to 0.408 kpc at $z_{src}=0.02$ and to 2.634 kpc at $z_{src}=0.15$.

2. Sample selection

We selected three radio galaxy catalogs to carry out our analysis, all obtained from the radio-loud sample of [Best & Heckman \(2012\)](#). All sources are selected on the basis of their morphology, as it is shown in the Faint Images of the Radio Sky at Twenty cm (FIRST) radio survey ([Becker et al. 1995](#)).

The first catalog is the WATCAT ([Missaglia et al. 2019](#)), listing 47 radio sources at low redshift ($z_{src} \leq 0.15$) showing two-sided jets with two clear warmspots (i.e., jet knots as bright as 20% of the nucleus) lying on the opposite side of the radio core and having classical extended emission resembling a plume beyond the warmspots. As shown in [Missaglia et al. \(2019\)](#), WATs show multifrequency properties remarkably similar to FR Is radio galaxies, being more powerful at radio wavelengths and similar to FR IIs. See Table A.1 for WATCAT sources radio luminosities at 1.4 GHz.

The second catalog is the combination of FRICAT and sFRICAT both described in [Capetti et al. \(2017a\)](#). FRICAT sources, chosen on the basis of their FR I radio morphology, are selected to have a radio structure extending beyond a distance of 30 kpc from the optical position of the host galaxy. The 14 sFRICAT sources have FR I radio morphology, whose radio emission extended between 10 and 30 kpc, and are limited to $z_{src} = 0.05$ (see [Capetti et al. 2017a](#), for details). The combination of these two samples includes FR Is at redshift $z_{src} \leq 0.15$. Sources from the FR I sample have radio luminosities at 1.4 GHz in the range $L_{1.4} \sim 10^{39.5} - 10^{41.3} \text{ erg s}^{-1}$ while sFR I radio luminosities spans $10^{39} - 10^{40.4} \text{ erg s}^{-1}$.

The third catalog is the FRIICAT ([Capetti et al. 2017b](#)), composed of 105 edge-brightened radio sources (FR II type) within the same redshift range of the previous catalog. Sources in this sample have radio luminosities at 1.4 GHz that cover the range $L_{1.4} \sim 10^{39.5} - 10^{42.5} \text{ erg s}^{-1}$.

All three catalogs include only sources lying in the footprint of the SDSS, that is also covered by the main catalog of groups and clusters of galaxies adopted in our analysis: the one created by [Tempel et al. \(2012\)](#), based on a modified version of the

Friends-of-Friends algorithm (Huchra & Geller 1982; Tago et al. 2010). The Tempel catalog has the largest number of galaxy cluster/group detections, with spectroscopic redshifts $0.009 \leq z_{cl} \leq 0.20$, with a peak around 0.08.

We want to stress that, thanks to the adopted selection criteria, all three radio galaxy catalogs are not contaminated by compact radio objects, as compact steep spectrum sources, and FR 0s (Baldi et al. 2015, 2018), which show a different cosmological evolution and lie in different environments.

3. Cosmological neighbors

To investigate the large-scale environment of WATs we first defined a type of optical sources: the *cosmological neighbors*.

We classify as cosmological neighbors all optical sources lying within a maximum distance of 2 Mpc radius computed at z_{src} of the central radio galaxy, with all the SDSS magnitude flags indicating a galaxy-type object (i.e., $uc=rc=gc=ic=zc=3$), and having a spectroscopic redshift z with $\Delta z = |z_{src} - z| \leq 0.005$. This value corresponds to $\sim 1500 \text{ km s}^{-1}$, that is the maximum velocity dispersion in groups and clusters of galaxies (see e.g., Berlind et al. 2006). However, in the galaxy-richest clusters, the large velocity dispersions may lead this method to underestimate the local galaxy density, due to some companion galaxies falling outside of the selected range.

We indicate as N_{cn}^{500} and N_{cn}^{2000} the number of cosmological neighbors lying within 500 kpc and 2 Mpc distance from the central radio galaxy, respectively, that provide an estimate of the environmental richness.

As shown in Fig. 1, it is quite evident that the N_{gal} parameter (cluster richness from Tempel et al. 2012) underestimates the group/cluster richness, and there are only a few cases in which N_{cn}^{2000} provides a lower estimate of the group/cluster richness.

4. Parameters definitions

Using the distribution of the cosmological neighbors it is possible to define several parameters that can be used to investigate the properties of the large-scale environments of WATs and

FR Is and FR IIs (hereinafter FRs). We thus defined the following quantities:

- The *average projected distance* d_{cn}^m that is average distance of the distribution of cosmological neighbors within 2 Mpc from the central radio source.
- The *standard deviation* σ_z of the redshift distribution of the cosmological neighbors surrounding each radio source within 2 Mpc.
- The *concentration parameter* ζ_{cn} , defined as the ratio between the number of cosmological neighbors lying within 500 kpc and within 1 Mpc. Under the assumption that the cosmological neighbours are uniformly distributed around the radio galaxy analyzed (given that the number of sources around a random position in the sky scales as $N \propto \vartheta^2$, where ϑ is the angular separation from the selected position) we should observe a value of ζ_{cn} equals 0.25. This parameter allows us to test if the radio galaxy analyzed tends to lie close to the center or in the outskirts of the group or clusters of galaxies in which it resides, if present.

All values of the environmental parameters for the WAT sample described above are reported in Table A.1 in Appendix.

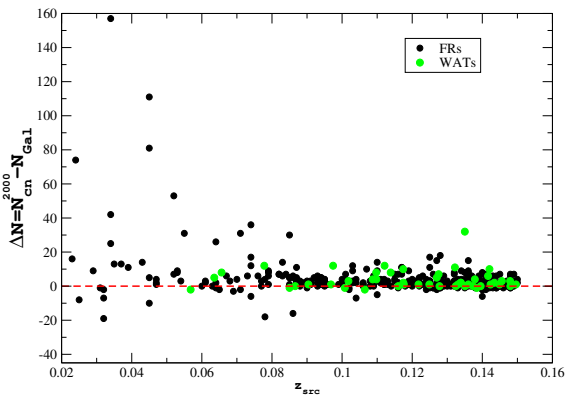


Fig. 1. The difference ΔN between the number of cosmological neighbors lying within 2 Mpc distance from the central radio source (N_{cn}^{2000}), and the richness estimated in the T12 cluster catalog (N_{gal}) as function of z_{src} . Grey circles mark radio sources in the FRICAT, sFRICAT and FRICAT, and green diamonds correspond to WATCAT sources.

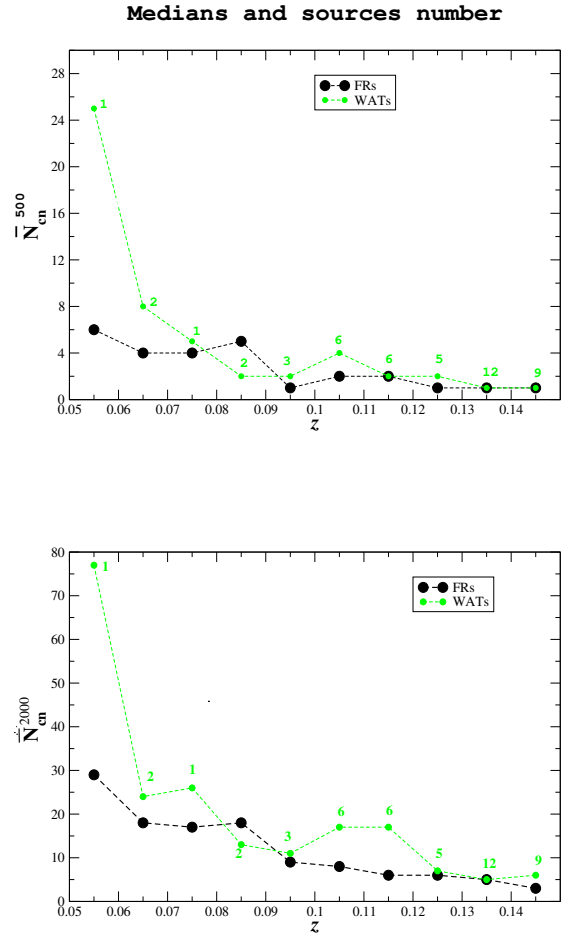


Fig. 2. Median values of the number of cosmological neighbors for the WATs (green) and the FRs (black) within 500 kpc (upper panel) and 2 Mpc (lower panel) per bin of redshift z . Above each median value we also report the number of sources in each bin of z starting from 0.05.

5. Statistical analysis

In this section we present the results obtained from the statistical analysis of WATs large scale environment by means of the environmental parameters previously defined, also searching for possible differences between WATs and FRs environmental properties.

In Fig. 2 we plot the medians of the number of cosmological neighbors within 500 kpc (upper panel) and 2 Mpc (lower panel) from the WATCAT sources. We can observe that median values for the WAT sample are systematically higher than that of FRs (with the only exception of the redshift bin 0.08-0.09). If we expect that medians for the WAT sample are distributed randomly, and therefore we have the same probability to find median values for WATs higher or lower than FRs one, according to the binomial distribution we find that the probability that WATs' N_{cn}^{500} are less than FRs' N_{cn}^{500} is $\sim 0.4\%$ and that WATs' N_{cn}^{2000} are less than FRs' N_{cn}^{2000} is $\sim 2\%$. Therefore we have some indications that WATs live in galaxy environments richer than that of FRs, but given the small sample of WATs the significance is too low to draw firm conclusions, even if we would expect richer environments, given the general consensus that WATs morphology is due to merger effects.

This result is in agreement with the results reported in Golden-Marx et al. (2021) for high- z bent radio sources, where the authors find that richer clusters host narrower bent radio sources.

Then we explore the distribution of the average projected distance d_{cn}^m of cosmological neighbors, which provides an estimate of the galaxy group/cluster physical size, as a function of the standard deviation σ_z of their redshifts (see Fig. 3 upper panel) and as a function of the redshift of the central source z_{src} , (see Fig. 3 lower panel) where we also overplot the mean value of the projected distance in each redshift bin of 0.01. In the left panel Fig. 3, we find that the standard deviation σ_z of cosmological neighbors' redshifts do not exceed a value of 0.003, that is consistent with the threshold of $\Delta z = |z_{src} - z| \leq 0.005$ used to select the cosmological neighbors, while in the right panel we find that all the sources in the WATCAT are clustered around a value of $d_{cn}^m \sim 1$ Mpc, implying that the size of the galaxy cluster/group in which the WAT is hosted is constant at low- z , and there are no values of d_{cn}^m larger than 1.2 Mpc, implying that WATs tend to occupy the central region of the galaxy group/cluster that inhabit. The observed scatter at high- z is due to the low number of cosmological neighbors detected. The same results are reported as normalized distributions in Fig. 4.

In Fig. 5 we show the distribution of the concentration parameter ζ_{cn} for WATCAT and FRs sources. If we assume that the cosmological neighbors are uniformly distributed around the radio galaxy analyzed, we should observe a value of $\zeta_{cn} = 0.25$. We obtain, instead, that the majority of the WATCAT sources (41 sources out of 47) have a value of ζ_{cn} higher than 0.25. This means that WATs tend to occupy the central region of the galaxy group/cluster in which they reside, in agreement with WATs being the BCGs. As shown in Golden-Marx et al. (2021) among the bent high- z radio sources considered in their study, some are indeed BCGs and others may evolve into BCGs. However, the lack of X-ray observation prevents us to compare the ICM morphology with the spatial distribution of the cosmological neighbors. As pointed out in Vardoulaki et al. (2019), the radio morphology, and in particular how the morphology is disturbed, can be used to identify possible X-ray group previously unidentified. As shown in Morris et al. (2022) bent sources are usually hosted in groups with an higher galaxy density with respect to that host-

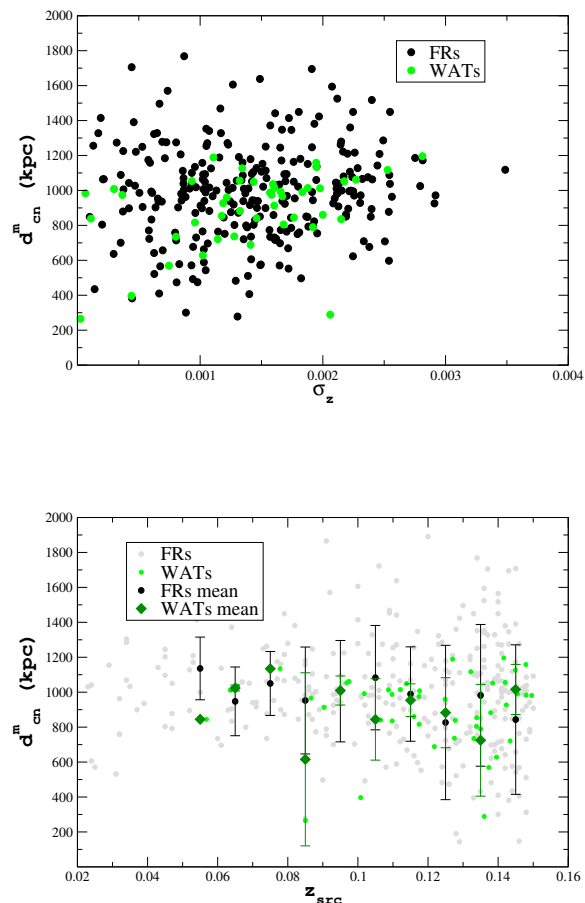


Fig. 3. Average projected distance d_{cn}^m of the distribution of cosmological neighbors as function of the standard deviation σ_z of their redshift distribution (upper panel) and of the redshift z_{src} of the central radio galaxy (lower panel). FR Is and FR IIs are indicated by black squares on the left and by gray squares on the right. WATCAT sources are in green. In the left panel we also show the results as mean values per redshift bin. WATs cosmological neighbors are clustered around $d_{cn}^m \sim 1$ Mpc. In the redshift bin 0.08-0.09 we observe a large scatter because we have only two sources with a large difference in the projected distance of the cosmological neighbors.

ing non-bent sources, and in general bent sources are hosted in environments that are larger, denser and less relaxed than unbent sources. As pointed out by the authors, also these results would benefit from X-ray observations, to trace the ICM responsible of the bending.

6. Summary and Conclusions

In this paper we presented an extensive investigation of WATs large-scale environment in the local Universe (i.e., at $z_{src} \leq 0.15$). Our analysis made use of cosmological neighbors, defined as optical sources lying within 2 Mpc from the target source, and with a redshift difference $\Delta z \leq 0.005$ with respect to the radio galaxy lying at the center of the field examined. In our study we also compared the large-scale environments of those radio galaxies classified as WATs with that of FR Is and FR IIs, all selected from extremely homogeneous catalogs, with uniform ra-

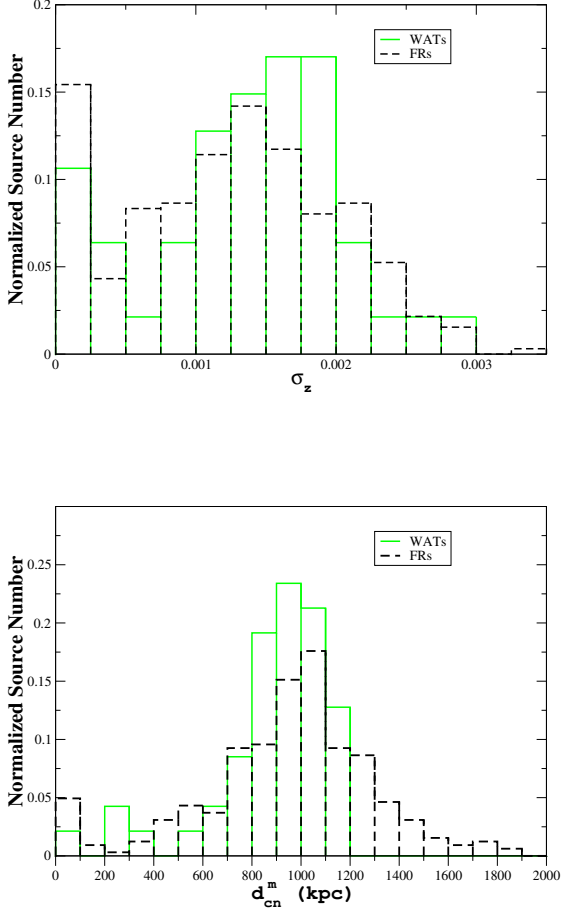


Fig. 4. Distribution of the standard deviation σ_z of their redshift distribution (upper panel) and of the average projected distance d_{cn}^m of the distribution of cosmological neighbors (lower panel).

dio, infrared and optical data available for all sources. For FR Is and FR IIs it has been found that, independently of their radio morphological classification, they all have environments that are indistinguishable. For this reason, we aimed at investigating the environmental properties of our sample with those already established for FR Is and FR IIs. We also want to stress that this analysis can not provide information on the intrinsic differences of the cluster hosting FRs and WAT, if any.

We emphasize the importance of *comparing radio sources in the same redshift bins* to obtain a complete overview of their large-scale environments, because this method takes into account cosmological biases.

Our main results are summarized as follows:

1. Median values of the number of cosmological neighbors within 500 kpc e 2 Mpc (N_{cn}^{500} and N_{cn}^{2000}) are systematically higher than those of radio galaxies within a level of confidence of 0.4% and 2%, depending on N_{cn}^{500} and N_{cn}^{2000} , respectively;
2. The average projected distance d_{cn}^m of the cosmological neighbors as function of the standard deviation σ_z of the redshift distribution of the cosmological neighbors and of the redshift z_{src} of the sources is clustered around a distance of ~ 1 Mpc, implying that in the redshift range explored, WATs

environments have similar sizes, and do not exceed 1.2 Mpc, while there is no trend observed for FR Is and FR IIs;

3. Typical values of the concentration parameter ζ_{cn} for WATs are well above 0.25 (it is ≥ 0.25 for 41 sources out of 47), value expected considering a uniform distribution of cosmological neighbors around the central RG, implying that WATs tend to inhabit the central region of the galaxy group/cluster in which they reside, therefore possibly being associated with the BCG of the galaxy group/cluster.

We plan to extend our sample with observations from low radio frequency telescopes, such as LOFAR and the uGMRT, augmented with the analysis of WATCAT X-ray observations, as the ones that eROSITA could provide in the upcoming future. We could therefore estimate properties of the ICM, such as X-ray luminosity L_X , mass and environmental mass M_{env} as well as X-ray fluxes. This information will complement the results obtained from the environmental parameters, given that both d_{cn}^m and ζ_{cn} traces the position of the mass, not the gas. We also want to highlight that we have explored any link between d_{cn}^m and σ_z in comparison with the absolute magnitude in the R band of the radio galaxy, but no trend/link is identified. A similar situation occurs also when comparing both these environmental parameters with radio power L_R and emission line luminosity of the [OIII], i.e., $L_{[OIII]}$. These results can be compared with that presented in Croston et al. (2019) for a sample of radio-loud AGN in the LOFAR Two-Metre Sky Survey (LoTSS) Data Release 1 catalogues. The authors find trends between the richness of the cluster and the radio luminosity, and also investigated the position of the sources with respect to the cluster centre. The absence of a trend in our sample could provide new insights on the different density of the environment observed for FRs and WATs.

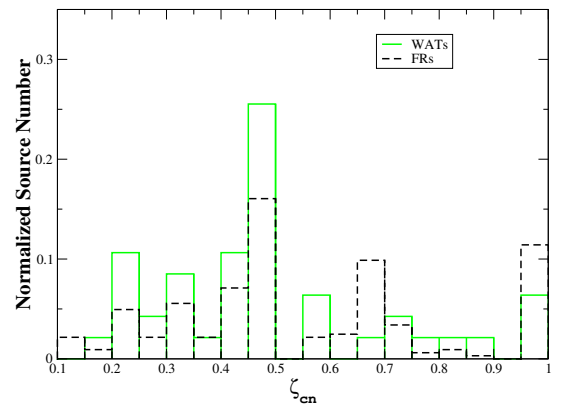


Fig. 5. The distribution of the concentration parameter ζ_{cn} estimated using the distribution of the cosmological neighbors. Black histogram refers to the FR I and FR IIs populations, and green one to WATs. The largest fraction of their values lie above the value of 0.25 expected assuming a uniform distribution of cosmological neighbors.

Appendix A: Table

We report here in Table A.1 all parameters used for the analysis of the WATs presented here.

We thank the anonymous referee for useful comments that led to improvements in the paper. F. M. wishes to thank Dr. C. C. Cheung for their valuable discussions on this project initially planned during the IAU 313 on the Galapagos islands. This work is supported by the “Departments of Excellence 2018 - 2022” Grant awarded by the Italian Ministry of Education, University and Research (MIUR) (L. 232/2016). This research has made use of resources provided by the Compagnia di San Paolo for the grant awarded on the BLENV project (S1618_L1_MASF_01) and by the Ministry of Education, Universities and Research for the grant MASF_FFABR_17_01. This investigation is supported by the National Aeronautics and Space Administration (NASA) grants GO4-15096X, AR6-17012X and GO6-17081X. F.M. acknowledges financial contribution from the agreement ASI-INAF n.2017-14-H.O. Funding for SDSS and SDSS-II has been provided by the Alfred P. Sloan Foundation, the Participating Institutions, the National Science Foundation, the U.S. Department of Energy, the National Aeronautics and Space Administration, the Japanese Monbukagakusho, the Max Planck Society, and the Higher Education Funding Council for England. The SDSS Web Site is <http://www.sdss.org/>. The SDSS is managed by the Astrophysical Research Consortium for the Participating Institutions. The Participating Institutions are the American Museum of Natural History, Astrophysical Institute Potsdam, University of Basel, University of Cambridge, Case Western Reserve University, University of Chicago, Drexel University, Fermilab, the Institute for Advanced Study, the Japan Participation Group, Johns Hopkins University, the Joint Institute for Nuclear Astrophysics, the Kavli Institute for Particle Astrophysics and Cosmology, the Korean Scientist Group, the Chinese Academy of Sciences (LAMOST), Los Alamos National Laboratory, the Max-Planck-Institute for Astronomy (MPIA), the Max-Planck-Institute for Astrophysics (MPA), New Mexico State University, Ohio State University, University of Pittsburgh, University of Portsmouth, Princeton University, the United States Naval Observatory, and the University of Washington. TOPCAT and STILTS astronomical software (Taylor 2005) were used for the preparation and manipulation of the tabular data and the images.

References

- Ascasibar, Y. & Markevitch, M. 2006, *ApJ*, 650, 102
 Baldi, R. D., Capetti, A., & Giovannini, G. 2015, *A&A*, 576, A38
 Baldi, R. D., Capetti, A., & Massaro, F. 2018, *A&A*, 609, A1
 Banfield, J. K., Wong, O. I., Willett, K. W., et al. 2015, *Monthly Notices of the Royal Astronomical Society*, 453, 2326
 Becker, R. H., White, R. L., & Helfand, D. J. 1995, *ApJ*, 450, 559
 Bennett, C. L., Larson, D., Weiland, J. L., & Hinshaw, G. 2014, *ApJ*, 794, 135
 Berlind, A. A., Frieman, J., Weinberg, D. H., et al. 2006, *ApJS*, 167, 1
 Best, P. N. 2004, *MNRAS*, 351, 70
 Best, P. N. & Heckman, T. M. 2012, *MNRAS*, 421, 1569
 Blanton, E. L., Gregg, M. D., Helfand, D. J., Becker, R. H., & Leighty, K. M. 2001, *AJ*, 121, 2915
 Blanton, E. L., Paterno-Mahler, R., Wing, J. D., et al. 2015, in *Extragalactic Jets from Every Angle*, ed. F. Massaro, C. C. Cheung, E. Lopez, & A. Siemiginowska, Vol. 313, 315–320
 Burns, J. O. 1981, *MNRAS*, 195, 523
 Capetti, A., Massaro, F., & Baldi, R. D. 2017a, *A&A*, 598, A49
 Capetti, A., Massaro, F., & Baldi, R. D. 2017b, *A&A*, 601, A81
 Carilli, C. L. & Barthel, P. D. 1996, *A&A Rev.*, 7, 1
 Croston, J. H., Hardcastle, M. J., Mingo, B., et al. 2019, *A&A*, 622, A10
 Fanaroff, B. L. & Riley, J. M. 1974, *MNRAS*, 167, 31P
 Garon, A. F., Rudnick, L., Wong, O. I., et al. 2019, *AJ*, 157, 126
 Giacintucci, S. & Venturi, T. 2009, *A&A*, 505, 55
 Golden-Marx, E., Blanton, E. L., Paterno-Mahler, R., et al. 2021, *ApJ*, 907, 65
 Gómez, P. L., Pinkney, J., Burns, J. O., et al. 1997, *ApJ*, 474, 580
 Hill, G. J. & Lilly, S. J. 1991, *ApJ*, 367, 1
 Huchra, J. P. & Geller, M. J. 1982, *ApJ*, 257, 423
 Longair, M. S. 1971, *Reports on Progress in Physics*, 34, 1125

- Massaglia, S., Bodo, G., Rossi, P., Capetti, S., & Mignone, A. 2019, *A&A*, 621, A132
- Massaro, F., Álvarez-Crespo, N., Capetti, A., et al. 2019, *ApJS*, 240, 20
- Miley, G. 1980, *ARA&A*, 18, 165
- Missaglia, V., Massaro, F., Capetti, A., et al. 2019, *A&A*, 626, A8
- Morris, M. E., Wilcots, E., Hooper, E., & Heinz, S. 2022, *AJ*, 163, 280
- O'Donoghue, A. A., Owen, F. N., & Eilek, J. A. 1990, *ApJS*, 72, 75
- Owen, F. N. & Rudnick, L. 1976, *ApJ*, 205, L1
- Prestage, R. M. & Peacock, J. A. 1988, *MNRAS*, 230, 131
- Smolčić, V., Schinnerer, E., Finoguenov, A., et al. 2007, *ApJS*, 172, 295
- Tago, E., Saar, E., Tempel, E., et al. 2010, *A&A*, 514, A102
- Taylor, M. B. 2005, in *Astronomical Society of the Pacific Conference Series*, Vol. 347, *Astronomical Data Analysis Software and Systems XIV*, ed. P. Shopbell, M. Britton, & R. Ebert, 29
- Tempel, E., Tago, E., & Liivamägi, L. J. 2012, *A&A*, 540, A106
- Vardoulaki, E., Jiménez Andrade, E. F., Karim, A., et al. 2019, *A&A*, 627, A142
- Wing, J. D. & Blanton, E. L. 2011, *AJ*, 141, 88
- Worrall, D. M. & Birkinshaw, M. 2000, *ApJ*, 530, 719
- York, D. G., Adelman, J., Anderson, John E., J., et al. 2000, *AJ*, 120, 1579
- Zirbel, E. L. 1997, *ApJ*, 476, 489

Table A.1. Properties of the WATCAT sources presented in this work with environmental parameters values.

SDSS name	z_{src}	$\log \nu L_\nu$	N_{cn}^{500}	N_{cn}^{2000}	ζ_{cn}	σ_z	d_{cn}^m
J004312.85-103956.0	0.12754	40.93	2.0	7.0	0.40	0.001	736.99
J080101.35+134952.2	0.10872	41.21	5.0	16.0	0.55	0.002	1013.38
J080337.67+105042.4	0.14234	40.98	1.0	4.0	0.33	0.001	927.21
J081803.86+543708.4	0.11742	41.43	7.0	28.0	0.5	0.002	975.40
J082718.31+463510.8	0.12487	40.74	2.0	9.0	0.33	0.001	959.80
J085116.24+082723.1	0.06354	40.36	7.0	15.0	0.87	0.002	1011.96
J091337.21+031720.5	0.14163	40.94	1.0	10.0	0.25	0.003	1195.88
J092428.89+141409.3	0.13842	40.44	5.0	33.0	0.42	0.002	1052.34
J092539.06+362705.6	0.11212	41.49	3.0	18.0	0.37	0.002	1015.23
J092612.34+324721.2	0.13953	41.38	3.0	4.0	1.0	0.001	628.37
J093349.82+451957.8	0.13387	41.33	1.0	4.0	0.5	0.001	854.25
J095716.41+190651.2	0.09039	40.88	2.0	11.0	0.29	0.002	913.53
J101932.33+140301.8	0.14558	41.33	4.0	10.0	0.80	0.002	989.99
J103502.62+425548.3	0.13602	40.86	2.0	3.0	0.67	0.002	288.96
J103605.76+000606.8	0.09683	41.25	0.0	3.0	0.0	9.32E-4	1053.76
J103636.24+383508.1	0.14489	41.14	0.0	3.0	0.0	0.001	1126.64
J103856.37+575247.5	0.10078	40.95	1.0	2.0	0.5	4.40E-4	396.52
J104645.86+314426.8	0.11386	40.81	2.0	16.0	0.28	0.001	1049.01
J104914.08+005945.2	0.10648	40.63	9.0	22.0	0.56	0.001	840.99
J114020.23+535029.1	0.14799	41.04	0.0	2.0	0.0	6.50E-5	983.40
J114111.81+054405.0	0.09743	41.24	13.0	57.0	0.59	0.002	1061.37
J115424.56+020653.0	0.13243	40.64	0.0	0.0	0.0	0.0	0.0
J115513.65-003133.9	0.13218	41.02	2.0	14.0	0.33	0.002	1117.27
J120118.19+061859.3	0.13505	40.54	1.0	3.0	0.5	3.66E-4	974.12
J120455.02+483256.9	0.06562	40.62	10.0	32.0	0.77	0.002	1035.64
J121439.53+052803.9	0.0778	40.13	5.0	26.0	0.5	0.002	1134.36
J130904.46+102935.3	0.08661	41.17	3.0	23.0	0.19	0.002	965.99
J133038.38+381609.7	0.10978	40.86	3.0	7.0	0.75	0.002	835.37
J135315.36+550648.2	0.14342	40.66	3.0	6.0	0.75	0.001	721.07
J141456.58+001223.0	0.12702	40.82	1.0	9.0	0.25	0.001	1189.28
J141513.98-013703.7	0.14959	41.24	0.0	1.0	0.0	0.0	981.44
J141718.94+060812.3	0.10972	40.91	3.0	17.0	0.30	0.002	987.50
J141731.27+081230.1	0.0568	40.58	25.0	77.0	0.48	0.002	844.98
J141927.23+233810.2	0.13732	40.12	1.0	2.0	0.5	7.45E-4	569.33
J143304.34+033037.6	0.14792	40.88	1.0	6.0	0.5	0.002	1158.48
J143409.03+013700.9	0.13786	41.61	2.0	9.0	0.40	0.001	882.68
J144700.45+460243.5	0.12777	41.04	1.0	2.0	1.0	1.10E-4	838.92
J144904.27+025802.7	0.12179	40.36	2.0	7.0	0.40	0.001	688.48
J150229.04+524402.0	0.13307	41.10	1.0	5.0	0.25	8.03E-4	734.93
J151108.77+180153.3	0.116	41.28	6.0	19.0	0.5	0.002	860.58
J154346.14+341521.6	0.11747	40.20	2.0	7.0	0.5	9.58E-4	816.44
J154729.59+145657.0	0.08501	40.69	2.0	2.0	1.0	2.50E-5	265.28
J155343.59+234825.4	0.11761	41.28	1.0	3.0	0.5	2.98E-4	1008.10
J161828.98+295859.6	0.13382	40.96	1.0	5.0	0.25	0.002	804.95
J164527.68+272005.8	0.10182	40.65	5.0	20.0	0.45	0.002	991.86
J212546.35+005551.8	0.13501	41.62	10.0	32.0	0.42	0.002	789.58
J222455.24-002302.3	0.14204	40.64	1.0	10.0	0.25	0.001	1056.20

Col. (1): SDSS name.

Col. (2): source redshift.

Col. (3): logarithm of the radio luminosity (erg s^{-1}).Col. (4,5): Number of cosmological neighbors within 500 and 2000 kpc, respectively, estimated at the z_{src} of the central radio galaxy.Col. (6): The concentration parameter ζ_{cn} .

Col. (7): The standard deviation of the redshift distribution for the cosmological neighbors within 2 Mpc.

Col. (8): Average projected distance of cosmological neighbors within 2 Mpc.